Fatigue behavior of woven-roving glass fiber reinforced-polyester under combined bending and torsional moments with different fluctuating stresses

M. Elhadary, M.N. Abouelwafa, A. Hamdy and T. Awad
Mechanical Eng. Dept., Faculty of Eng., Alexandria University, Alexandria, Egypt

The fatigue behavior of woven-roving glass fiber reinforced polyester (GFRP) was studied under combined bending and torsional moments, in-phase, with different fluctuating stresses. Fatigue tests were conducted on two fiber orientations, $[0,90]_2$ and $[\pm45]_2$, thin-walled tubular specimens with different ratios of the flexural stress (A) to the torsional stress (B) , these ratios were A/B = 0.5, 1, 2. To study the effect of mean stress of fatigue behavior, specimens were fatigue tested at different stress ratios ($R=\frac{\min.stress}{\max.stress}$), R = -1 ,-0.75, -0.5, -0.25, 0 for $[0,90]_2$ specimens with A/B=2 and R = -1 , -0.75, -0.5, -0.25 for $[\pm45]_2$ specimens with A/B= 1. The results showed that the $[\pm45]_2$ woven-roving GFRP is more fatigue resistant in torsion than the $[0, 90]_2$, while the $[0, 90]_2$ woven-roving GFRP is more fatigue resistant in bending than the $[\pm45]_2$. The form as Goodman's equation $\left\{\frac{\sigma_m}{S_u}+\frac{\sigma_a}{S_f}=1\right\}$ was found to be suitable for representing the effect of the mean stress for both orientations, $[0, 90]_2$ and $[\pm45]_2$, under combined bending and torsional fatigue loading. A new form of failure criteria was introduced to govern the fatigue behavior of studied case, considering the interact effect between the local stresses and taking into account the variations of the values of (R) and (A/B) ratios.

تم دراسة سلوك الكلال فى البوليستر المدعم بالألياف الزجاجية المنسوجة شبكيا والمؤثر عليه بإجهادات مركبه مكونه من عزوم إنحناء وإلتواء بنفس الطور فى وجود أحمال متغيرة مختلفة. إجريت إختبارات الكلال على اتجاهين مختلفين من التدعيم فى العينات وهما [صفر، ٩٠] و[٤٥،- ٤٥] تحت تأثير نسب مختلفة من إجهاد الإنحناء(A)إلى إجهاد القص(B). هذة النسب كانت A/B = ٠،٥ ، ١ ، ٢. ولدراسة تأثير وجود أحمال متوسطة على سلوك الكلال، إختبرت عينات عند نسب إجهادات مختلفة (R= الإجهاد الأدنى / الإجهاد الأقصى) كالأتى: R= - ١، - ٧٥،، - ٥،، - ٢٥،، صفر للإتجاة [صفر، ٩٠] عند قيمة A/B = ٢ وللإتجاه [٤٥،- ٤٥] اختبرت عند R= - ١ ، - ٧٥, ، - ٥،، - ٢٥, عند قيمة A/B = ١. أظهرت النتائج أن الإتجاة [٤٥،- ٤٥] كان أكثر تحملاً لحمل الكلال تحت تأثير عزم الإلتواء بمفردة من الإتجاة [صفر، ٩٠] . بينما فى حالة حمل الكلال تحت تأثير عزم الإنحناء بمفردة كانت العينات ذات الإتجاة [صفر، ٩٠] اكثر مقاوماً من الإتجاة [٤٥،- ٤٥]. كما أوضحت النتائج أن الصورة العامة لمعادلة Goodman $\left\{\frac{\sigma_m}{S_u}+\frac{\sigma_a}{S_f}=1\right\}$ تعبر عن تاثير الإجهادات المتوسطه وذلك بالنسبة للإتجاهين [صفر، ٩٠] و[٤٥،- ٤٥]وذلك تحت أحمال مجمعه من عزوم الإنحناء و الإلتواء المتغيرين.أيضا اقترحت الدراسة تعديل لنظريات الإنهيار المختارة لتلائم سلوك الكلال فى حالة التجارب الحالية والتى تأخذ فى الإعتبار تأثير التداخل بين الإجهادات المحلية المختلفة وكذلك التغير فى قيم النسب (R) ، (A/B).

Keywords: Fatigue, Glass fiber, Polyester, Combined moments, Fluctuating stresses

1. Introduction

The fatigue behaviour of composite materials, which are inhomogeneous and anisotropic, is more complicated than that of homogeneous and isotropic materials such as metals. In metals, the stage of gradual and invisible deterioration spans nearly the complete lifetime. No significant reduction of stiffness is observed during the fatigue process. The final stage of the process starts with the formation of small cracks; gradual growth and coalescence of these cracks quickly produce a large crack and final failure of the structural component. As the stiffness remains unaffected, the fatigue process can be

simulated by a linear elastic analysis and linear elastic fracture mechanics. In composite materials, damage starts very early and the extent of the damaged zones grows steadily. The gradual deterioration, with a loss of stiffness in the damaged zones, leads to a continuous redistribution of stress and may lead to a reduction of stress concentrations inside a structural component. As a consequence a prediction of the final state requires the simulation of the complete path of successive damage states.

Wang S.S. et al. [1] studied the fatigue behavior of G-10 grade glass fiber-reinforced composite laminates subjected to cyclic uniaxial tensile and pure torsion at cryogenic temperatures. They used two fiber orientations $[0, 90]_{2s}$, $[\pm45]_{2s}$. Their conclusions may be summarized as follows:

1. Torsion fatigue loading places severe shear stress on the composite; fatigue resistance in this condition is lower than that in a tensile mode in general.
2. Fatigue degradation of composite laminated at cryogenic temperature may be related to the change of material stiffness. The axial stiffness reduction in $[\pm45]_{2s}$ composite laminates under uniaxial tensile fatigue is more severe, and the rate of degradation is more rapid than in $[0, 90]_{2s}$ laminates under the same loading mode.

Kremple E. et al. [2] tested graphite/epoxy thin-walled tubes under uniaxial and biaxial loading and for negative stress ratios. The in-phase biaxial fatigue tests were conducted on specimens with [0/45] fiber orientation and at R= -1, with a different magnitudes of axial to torsional stress ratio loadings. The results served in plotting S-N curves, where the fatigue curve was found to be much steeper than observed under uniaxial loading. The fatigue strength amplitude at 10^6 cycles estimated to be only one third of the ultimate tensile strength.

EL-Midany A.A. [3] studied the biaxial fatigue of woven-roving glass Giber Reinforced Polyester (GRP) subjected to in-phase and out-of-phase cyclic bending and tensional loadings, conducted his tests on two fiber orientations $[0, 90]_2$ and $[\pm45]_2$ thin-walled tubes. His results showed that:

- The $[0, 90]_2$ woven-roving GRP is more fatigue resistance in bending than the $[\pm45]_2$ tubes.
- The $[\pm45]_2$ woven-roving GRP is more fatigue resistance in torsion than the $[0, 90]_2$ tubes.
- For in-phase loading, as well as, out-of-phase loading, at bending to torsion ratios less than 2; the $[\pm45]_2$ specimens are much stronger than the $[0, 90]_2$ specimens, while at bending to torsion ratio equal to 2; both types of specimens had nearly the same fatigue strength.

Bradley A. Lerch [4] studied the fatigue behavior of unidirectional SiC/Ti-15-3 composite under both tension and compression with different mean stresses. He found that the tensile mean stresses were detrimental and that compressive mean stresses were beneficial to the fatigue strength, which was similar to their effects on the fatigue behavior of metals.

Mohamed N.A. [5] tested woven-roving GFRP specimens with $[0, 90]_2$ and $[\pm45]_2$ fiber orientations under torsional fatigue loading with different mean stresses. He found out some important conclusions that may be summarized as follows:

- The mean-stress component is ineffective for specimens under pure local shear stress, $[0, 90]_2$ fiber orientation, to a certain ratio, then the mean stress component is found to have a detrimental effect on the amplitude component for the same life.
- When specimens were subjected to tension-compression local stress components, $[\pm45]_2$ fiber orientation, the mean stress was found to have a detrimental effect for all negative stress ratios, and the classical Goodman's equation for normal stresses replaced by the corresponding shear stresses was found to Govern the Fatigue Behaviour of woven-Roving (GFRP).

2. Experimental work

2.1. Specimens

2.1.1. Materials

The specimens were made from woven-roving E-glass fibers and polyester resin. Table 1 shows the properties of the tested materials. The trade name of polyester resin

used in the present work is "siropol 8330 [3, 5, 8, 6, 7]. This resin was prepromoted with Cobalt Naphthenate (6%solution), as an accelerator in percentage of 0.2 % by volume, and Methyl Ethyl Ketone (M.E.K.) peroxide as a catalyst in a percentage of 2% by volume. The volume fraction (V_f) has a great effect on mechanical properties of composites. In the present work, the volume fraction (V_f) ranges from 55% to 65%; because this range has proved its suitability to ensure specimens with good strength, good adhesion between fibers and matrix, and acceptable mechanical properties [3, 5, 7].

2.1.2. Shape and dimensions

The available testing machine was designed to test tubular specimens. So, thin wall tubular specimens were used for the experimental work to ensure having a plane uniform stress. A schematic drawing for this procedure is shown in fig. 1. The dimensions of the specimens used in the present work are within the standard dimensions and similar to those used by pervious investigators [3, 5, 8]. To avoid the failure of some specimens at the end of the gauge length, beneath the grippers, two wooden plugs were inserted into the specimens from both ends. And an elastic sleeve was shrinked on the outer surface at both ends.

2.2. Testing machine

The used testing machine was previously designed, with the principal of controlled strain, by Abouelwafa M.N. et al. [9] and used by other researchers [3, 5, 6-8] in similar work. The general layout is shown in fig. 2.

This testing machine is rotating with constant speed of 8.75Hz (525 r.p.m.) and provides three different fatigue-loading systems pure bending, pure torsion, and combined bending and torsion, independently, whether in-phase or out-of-phase. These loading systems gave the opportunity to apply different mean stresses. Details of the machine operation and loading systems were given by [3].

2.3. Stress state

The global stresses resulted from bending and tosional moments may be found from the following equations:

$$\sigma_x = \frac{My}{I},\ \sigma_y = 0.0,\ \tau_{xy} = \frac{Tr}{J}.$$

Where:

M is the applied bending moment , $(M = M_m + M_a \sin(\omega t))$,

T is the applied torque $(T = T_m + T_a \sin(\omega t))$,

M_m, M_a, T_m T_a are the mean and amplitude bending and torsional moments, respectively,

(ωt) is the twisting angle,

I is the second moment of area,

J is the second polar moment of area,

d_o, d_i are the outer and inner diameters of the specimen, respectively,

I is the $\frac{\pi}{64}(d_0^4 - d_i^4)$, $J = \frac{\pi}{32}(d_0^4 - d_i^4)$, and

Y is the $r = \frac{d_o}{2}$.

The local stresses for $[0, 90]_2$ specimens were $\sigma_1 = \sigma_x, \sigma_2 = 0,$ and $\sigma_6 = \tau_{xy}$, while for $[\pm 45]_2$ specimens were $\sigma_1 = \frac{\sigma_x}{2} + \tau_{xy}, \sigma_2 = \frac{\sigma_x}{2} - \tau_{xy},$ and $\sigma_6 = -\frac{\sigma_x}{2}$

3. Test results

It is important to note that, in order to avoid any misleading data, only the specimens that had their failure features within the accepted gauge section, the middle third of the whole length, were considered; while those that seemed to have their failure due to any gripping problems were excluded. Each experimental data point was obtained by considering the average of three specimens tested under the same conditions.

Most researchers use the stress Ratio (R) when dealing with the effect of mean stress

Table 1
Properties of used materials

Woven–roving E-glass fibres		Polyester	
Property	Value	Property	Value
Density	2551 kg / m^3	Density	1161.3 kg / m^3 (measured)
Modulus of elasticity	E = 76 GPa	Modulus of elasticity	E = 3.5 GPa
Poisson's ratio	υ = 0.37	Poisson's ratio	υ = 0.25
Tensile strength	3.45 GPa	Gel time at 25 °C	20 min.
Average mass / area	600 gm / m^2	Viscosity	0.45 Pa.s
Average thickness	0.69 mm	Percentage of Styrene	40 %

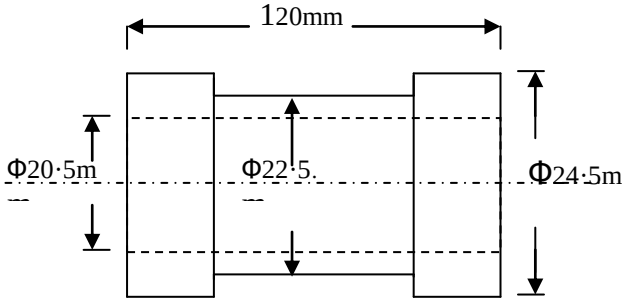

Fig.1. Dimensions of used specimens.

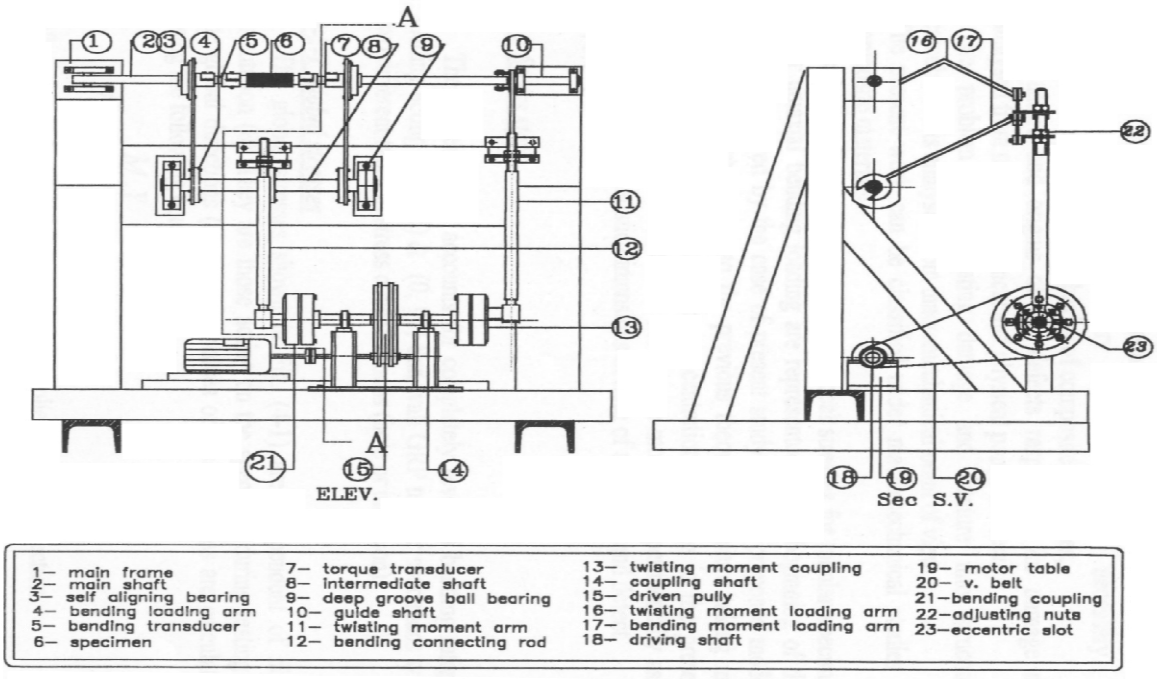

Fig. 2. General layout of the testing machine.

3.1. Static tests

Static bending and torsional tests were conducted on the specimens of both orientations $[0, 90]_2$ and $[\pm45]_2$ to find out their ultimate global bending (S_U) and shear strengths (S_{US}).

3.2. Fatigue tests

More than 400 test specimens were fatigue tested in-phase under ambient conditions and constant frequency of 8.75 Hz. For each orientation $[0, 90]_2$ and $[\pm45]_2$, the data points were used to plot the corresponding S-N curves on a semi-log scale, being fitted using the power low; Max. Stress = a N^b. Failure was considered to occur when the load reading decreased by about 20% of its original value. In other words, 20 % reduction in the strength of the specimen will represent failure.

3.2.1. Pure bending

The data points of the completely reversed pure bending tests of $[0, 90]_2$ and $[\pm45]_2$ were plotted in fig. 3. It is important to note that, the global fatigue bending strength of the $[0, 90]_{2S}$ tubes is considered as the local fatigue strength of the woven-roving GFRP in the fiber direction (F_1).

3.2.2. Pure torsion

The data of the tested conducted on $[0, 90]_2$ and $[\pm45]_2$ specimens, subjected to completely reversed pure torsion were plotted in fig. 4.

3.2.3. Combined bending and torsion

Theses results were divided into two groups as following:

1. For R = -1, $[0, 90]_2$ and $[\pm45]_2$ specimens were tested under combined bending and torsional moments with A/B ratios of 0.5, 1, 2. Figs. 5 to 9 were plotted with the vertical axis representing the maximum normal stress, where the value of corresponding maximum shear stress may be calculated using the ratio A/B.

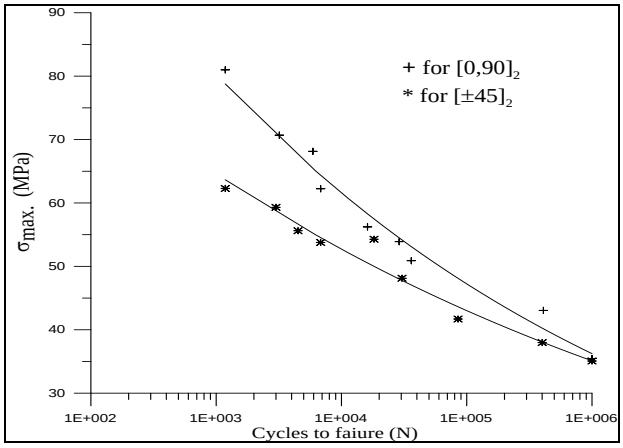

Fig. 3. Completely reversed pure bending S-N curve of $[0, 90]_2$ and $[\pm45]_2$ specimens.

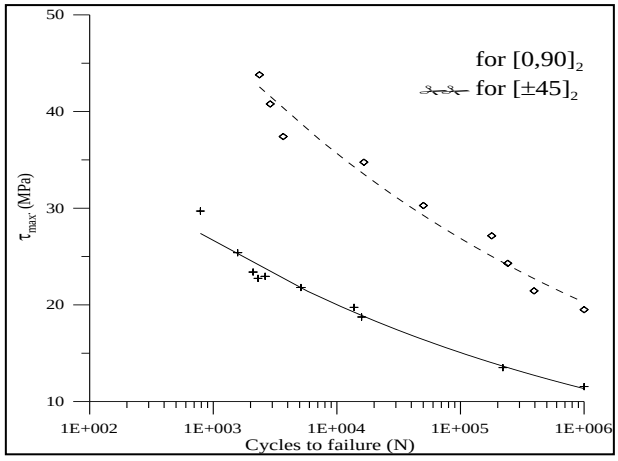

Fig. 4.Completely reversed pure torsion S-N curve of $[0, 90]_2$ and $[\pm45]_2$ specimens.

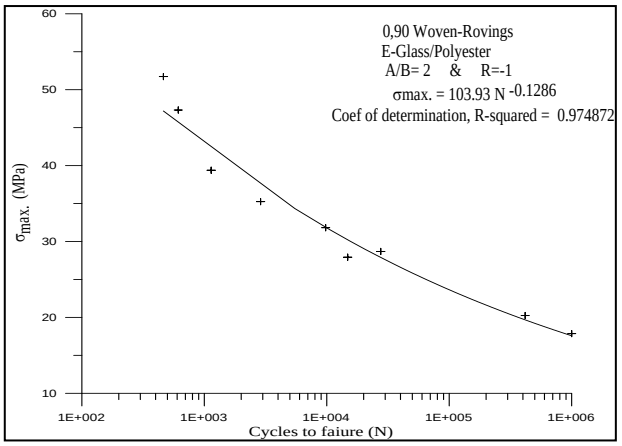

Fig. 5. S-N curve of $[0, 90]_2$ specimens tested under A/B=2 and R=-1.

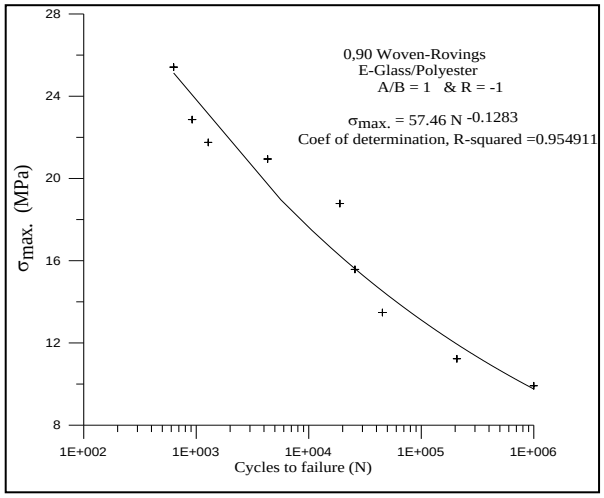

Fig. 6. S-N curve of $[0, 90]_2$ specimens tested under A/B=1 and R=-1.

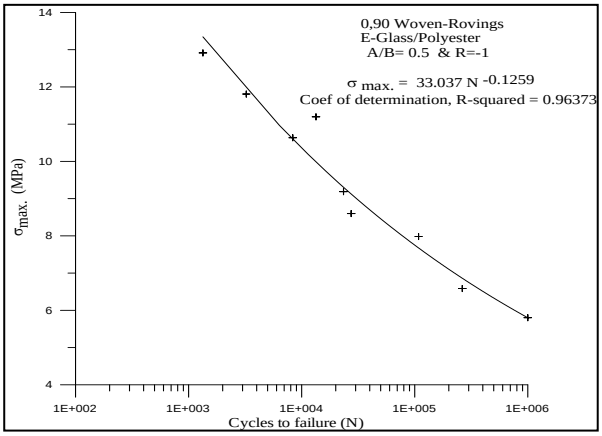

Fig.7. S-N curve of $[0, 90]_2$ specimens tested under A/B=0.5 and R=-1.

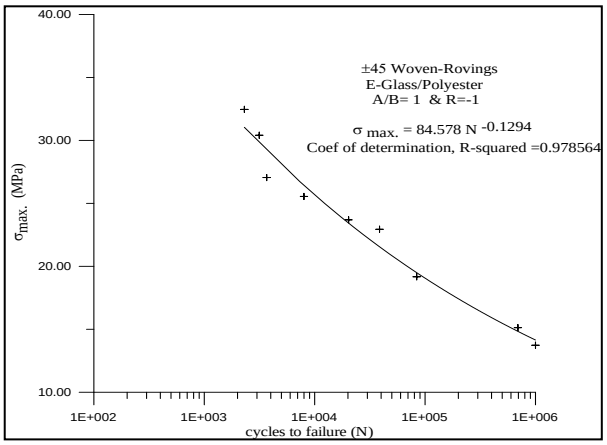

Fig. 8. S-N curve of $[\pm45]_2$ specimens tested under A/B=1 and R=-1.

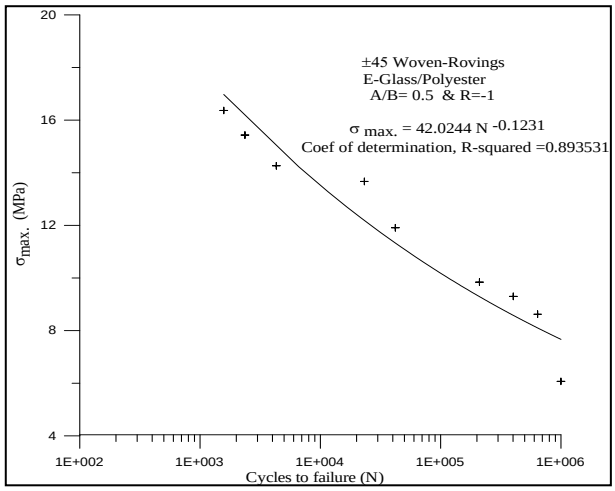

Fig. 9. S-N curve of $[\pm45]_2$ specimens tested under A/B=0.5 and R=-1.

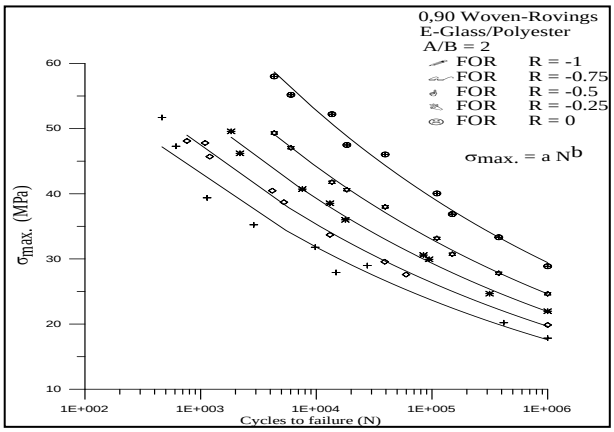

Fig. 10. S-N curve for $[0, 90]_2$ specimens at all stress ratios with A/B=2.

3. In order to study the effect of mean stress, tested were performed on both fiber orientations, $[0, 90]_2$ and $[\pm45]_2$, at five different stress ratios (R = -1, -0.75, -0.5, -0.25, 0). Fig. 12 shows the corresponding S-N curve for $[0, 90]_2$ at all stress ratios with A/B=2, while fig. 13 is for $[\pm45]_2$ at A/B=1. The two constants (a and b), of the used power law, $\sigma_{Max.} = a\, N^{b}$, for $[0, 90]_2$ and $[\pm45]_2$ specimens are found in tables 2 and 3, respectively.

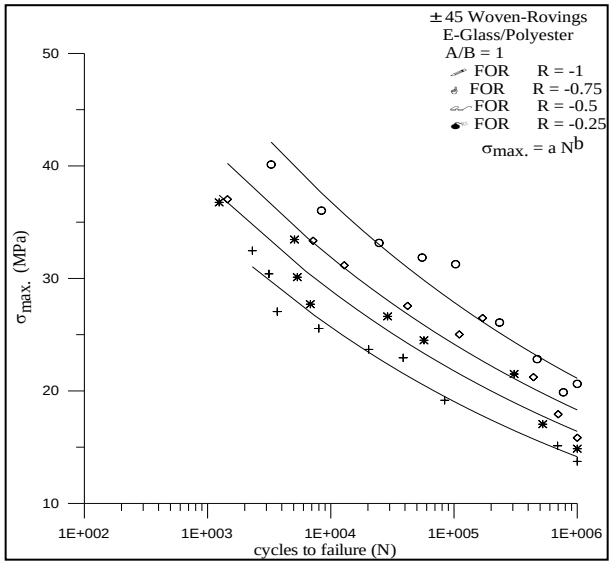

Fig. 11. S-N curve for $[\pm45]_2$ specimens at all stress ratios with A/B=1.

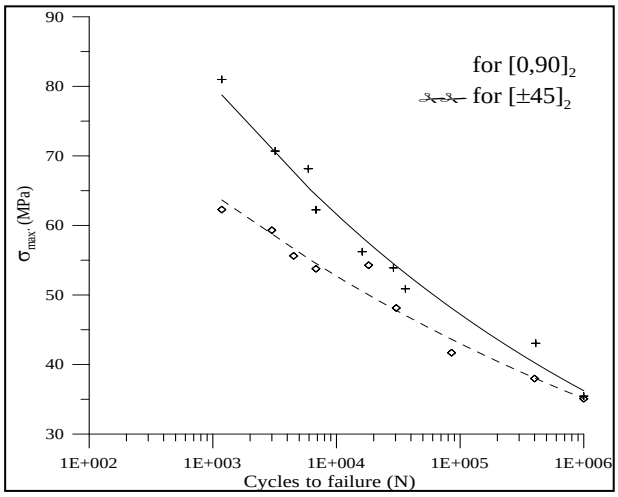

Fig. 12. Completely reversed pure bending S-N curve of $[0, 90]_2$ and $[\pm45]_2$ specimens.

Table 2
Fatigue constants (a and b) of $[0, 90]_2$ specimens with A/B=2

Stress ratio (R)	a. (MPa)	b.	Correlation factor
-1	103.93	-0.1286	0.9748
-0.75	113.92	-0.1271	0.9967
-0.5	126.11	-0.1266	0.994
-0.25	141.85	-0.1267	0.9965
0	170.17	-0.1265	0.9837

Table 3
Fatigue constants (a and b) of $[\pm45]_2$ specimens with A/B=1

Stress ratio (R)	a. (MPa)	b.	Correlation factor
-1	84.578	-0.1294	0.978
-0.75	89.94	-0.1231	0.937
-0.5	96.66	-0.1204	0.9042
-0.25	111.86	-0.1207	0.9363

4. Analysis and discussion

4.1. Analysis of S-N curves

From the results of tests conducted under completely reversed pure bending and completely reversed pure torsion, one can notice that the $[0, 90]_2$ specimens have higher bending strength than the $[\pm45]_2$ specimens.

While the $[\pm45]_2$ specimens have higher torsional strength than the $[0, 90]_2$ specimens as shown in figs. 12 and 13.This was also found in many other researches [1, 3, 5, 7, 8, 10].

This conclusion may be explained considering the local stress state;

- In case of completely reversed pure torsion, the $[\pm45]_2$ specimens were subjected to tension-compression $(\sigma_1 = -\sigma_2 = \tau_{xy}, \sigma_6 = 0)$, while the $[0, 90]_2$ specimens were subjected to pure shear $(\sigma_1 = \sigma_2 = 0, \sigma_6 = \tau_{xy})$. The tension or compression component found in $[\pm45]_2$ specimens are supported by fiber, while for the $[0, 90]_2$ specimens under torsional fatigue; matrix-dominated damage by interference debonding and matrix cracking prevails [1].
- In completely reversed pure bending case, the $[0, 90]_2$ specimens are subjected to only tension stress in fiber direction $\sigma_1 = \sigma_x, \sigma_2 = \sigma_6 = 0$), while the $[\pm45]_2$ specimens are subjected to tension in both fiber directions and shear stress $(\sigma_1 = \sigma_2 = \frac{\sigma_x}{2}, \sigma_6 = -\frac{\sigma_x}{2})$. The reason is that the tensile stresses acting perpendicular and along the fibers in presence of the shear stress help the cracks initiated in the matrix, tangentially to the fibers, to propagate as interfacial shear mode [3].

Using the power formula: $\sigma_{max.} = a\ N^b$ has proven its suitability by giving excellent fitting. Comparing the values of the constant (a) resulted in the following conclusions:
- The value of the constant (a) was found to depend on the (A/B) ratio for both fiber orientations according to the following equations:

$$a_{[0,90]_2} = 16.08 Ln(\frac{A}{B}) + 67.07$$

$$a_{[\pm 45]_2} = 13.61 Ln(\frac{A}{B}) + 69.88$$

Decreasing the value of (A/B) causes a decrease in the corresponding value of (a). This was due to the dominated failure mode was matrix mode and by decreasing the value of (A/B) the local shear stress increases.

4.2. Effect of mean stress

Analyzing the values of two constants (a) and (b) of the data considering the variation of stress ratios, resulted in the following conclusions:
1. The deviation in the values of the power (b) at different stress ratios is negligible and it may be considered to be constant, considering each of $[0, 90]_2$ and $[\pm 45]_2$ specimens separately, the average value of (b) was calculated and considered to be used at any stress ratio, as the corresponding standard deviation was found to have acceptable values.
2. The value of the constant (a) was found to depend on the stress ratio (R) for both fiber orientations, as the following relations:

$$a_{[0,90]_2\left(\frac{A}{B}=2\right)} = 64.16 * R + 163.28$$

$$a_{[\pm 45]_2\left(\frac{A}{B}=1\right)} = 35.4 * R + 117.9$$

Increasing the value of (R) causes an increase in the corresponding value of (a); i.e. the fatigue strength increases with the increase of (R).

The need for groups of specimens, one at each stress ratio, having exactly the same life; make it impossible to use the actual experimental data in plotting the mean – amplitude relations. So, we used the fitted (S-N) equations to find out the required points. The mean – amplitude diagrams were plotted at different lives for each of the $[0, 90]_2$ and $[\pm 45]_2$ specimens, as shown in figs. 16 and 17.

plotting the mean-amplitude components of the $[0, 90]_2$ and $[\pm 45]_2$ specimens representing the negative stress ratios and using the static point (S_U, 0) gave straight line relations, with high correlation factors. Since at any life, the fitted straight line joins the two points (S_U, 0) and (0, S_F) and passes by the other points with a high correlation factors, this supports the use of an equation in the form as Goodman's equation to be governing the mean-amplitude relation.

Therefore, the equation: $\left\{\frac{\sigma_m}{S_u} + \frac{\sigma_a}{S_f} = 1\right\}$ is suitable for representing the effect of the mean stress for both orientations, $[0, 90]_2$ and $[\pm 45]_2$, under combined bending and torsional fatigue loading.

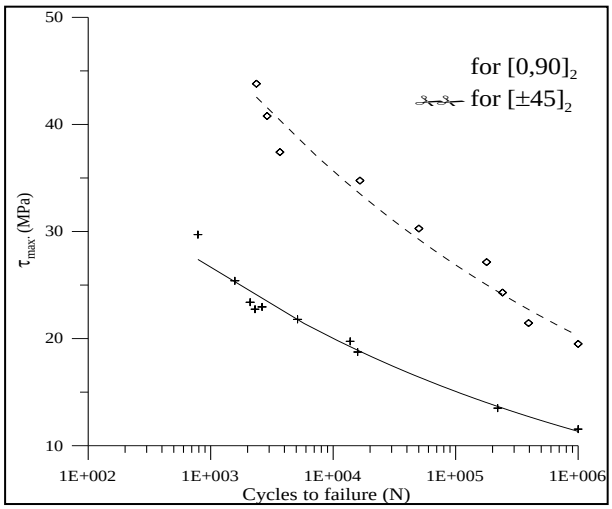

Fig.13. Completely reversed pure torsion S-N curve of $[0, 90]_2$ and $[\pm 45]_2$ specimens.

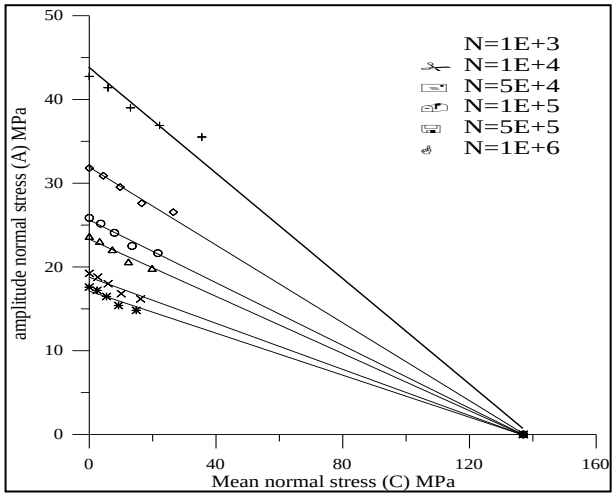

Fig. 14. Mean-Amplitude calculated for the $[0, 90]_2$ specimens with (A/B = 2).

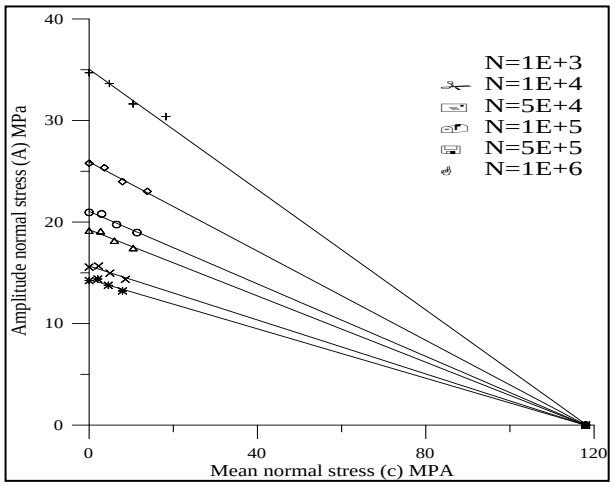

Fig. 15. Mean-Amplitude calculated for the $[\pm 45]_2$ specimens with (A/B = 1).

4.3. Applicability of failure criteria

All failure criteria have their right hand side to be unity and the left hand side contains the local stress components divided by their corresponding strength. To evaluate the validity of the failure criteria, we shall consider the right hand side of the failure criteria as a Relative Damage (RD). The relation between the RD with number of cycles to failure (N) is plotted for different failure criteria. In these curves as much as RD is close to unity, this means that the criterion is suitable. If it is less than unity, then the criterion is predicting a specimen life more than the actual life of the experimental results. Many previous works [1, 3, 5, 7, 8, 10], had been done considering the suitability of failure criteria to similar materials with same orientations. Considering these works, it was found that the most extensively used and suitable criteria for GFRP under different loading conditions were the following:

- Hill $\left(\frac{\sigma_1}{F_1}\right)^2+\left(\frac{\sigma_2}{F_2}\right)^2+\left(\frac{\sigma_6}{F_6}\right)^2-2\left(\frac{\sigma_1\sigma_2}{F_1F_2}\right)=1$

- Tsai-Wu

$$\left(\frac{\sigma_1}{F_1}\right)^2+\left(\frac{\sigma_2}{F_2}\right)^2+\left(\frac{\sigma_6}{F_6}\right)^2+2\left(\frac{\sigma_1\sigma_2}{F_1F_2}\right)=1$$

- Cowin

$$\left(\frac{\sigma_1}{F_1}\right)^2+\left(\frac{\sigma_2}{F_2}\right)^2+\left(\frac{\sigma_6}{F_6}\right)^2+2\sigma_1\sigma_2\left(\frac{1}{F_1F_2}-\frac{1}{2F_6^2}\right)=1$$

- Norris and McKinnon

$$\left(\frac{\sigma_1}{F_1}\right)^2+\left(\frac{\sigma_2}{F_2}\right)^2+\left(\frac{\sigma_6}{F_6}\right)^2=1$$

- Tsai-Hahn, Tsai-Hill, and Norris distortional energy have the same form for woven-roving with equal fiber intensity in both directions.

$$\left(\frac{\sigma_1}{F_1}\right)^2+\left(\frac{\sigma_2}{F_2}\right)^2+\left(\frac{\sigma_6}{F_6}\right)^2-\left(\frac{\sigma_1\sigma_2}{F_1F_2}\right)=1$$

The local stress components of the $[0, 90]_2$ specimens, $(\sigma_1=\sigma_x, \sigma_2=0, \sigma_6=\tau_{xy})$, were substituted in the pervious failure criteria; this substitution has shown that all failure criteria have the same form as following:

$$\left(\frac{\sigma_1}{F_1}\right)^2+\left(\frac{\sigma_6}{F_6}\right)^2=RD$$

Fig. 16 represents the relative damage for the $[0, 90]_2$ specimens under completely reversed combined fatigue loading with $A/B = \frac{0}{1}$, 0.5, 1, 2, $\frac{1}{0}$, and also for A/B = 2 with

different stress ratios (R = -0.75,-0.5, -0.25,0), against the number of cycles to failure. The values of RD is ranging from 0.73 as a minimum value to 1.4 as a maximum value. This means that, the available different failure criteria are not suitable under theses conditions and must be modified to best suit the studied case.

The relative damage RD were calculated, according to the pervious failure criteria, for the $[\pm 45]_2$ specimens under completely reversed combined fatigue loading with A/B = $\frac{0}{1}$, 0.5, 1, 2, $\frac{1}{0}$, and also for A/B = 1 with different stress ratios (R = -0.75,-0.5,-0.25), and plotted against the number of cycles to failure as shown in figs. 17 to 20.

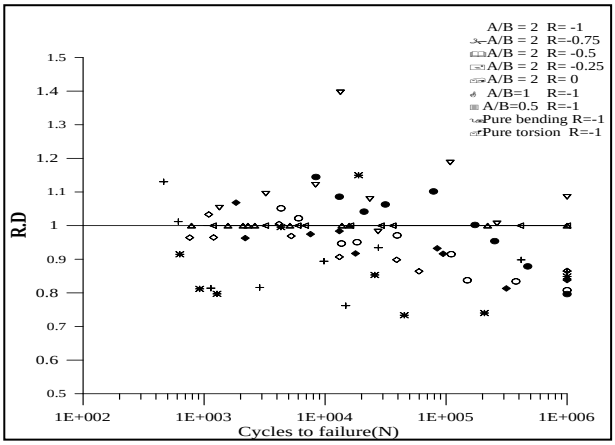

Fig. 16. R.D. of all failure criteria for the $[0, 90]_2$ specimens.

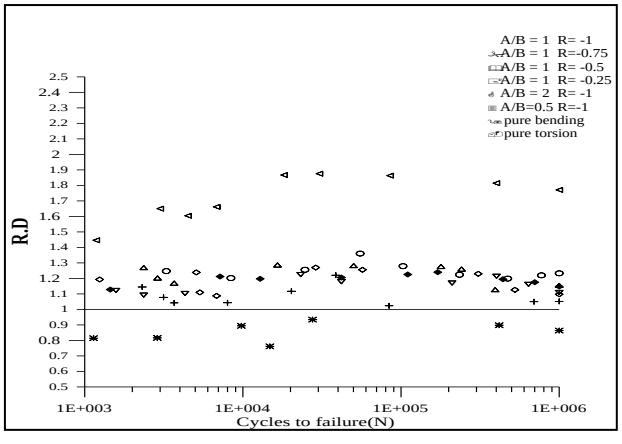

Fig. 17. Relative damage RD applying Hill failure criterion for the $[\pm 45]_2$ specimens.

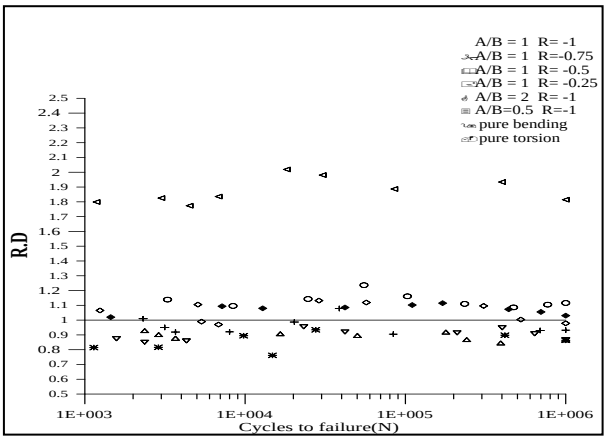

Fig. 18. Relative damage RD applying Tsai-Hahn criterion for the $[\pm 45]_2$ specimens.

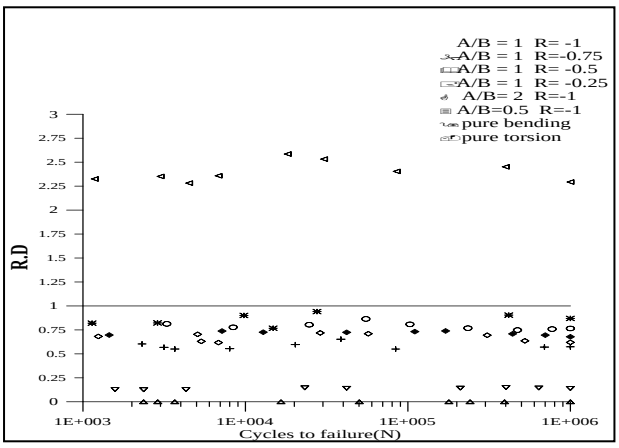

Fig. 19. Relative damage RD applying Tsai-Wu criterion for the $[\pm 45]_2$ specimens.

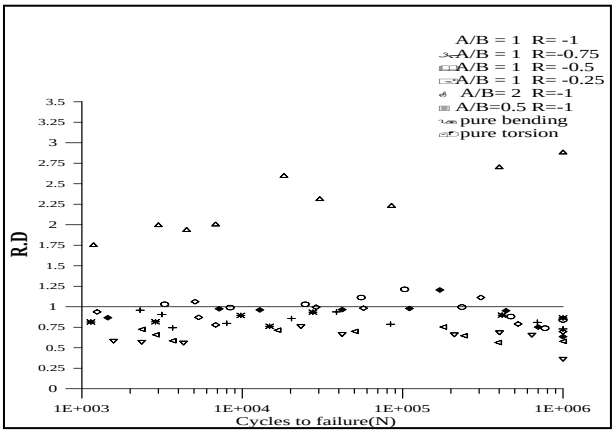

Fig. 20. Relative damage RD applying Norris and McKinnon criterion for the $[\pm 45]_2$.

Figs. 16 to 20 show that the values of RD for different selected failure criteria were found to be far from the unity. Therefore, these criteria should be modified to best suit with the studied case. A new terms were introduced to increase the correlation between the experimental data and theoretical equations. These terms were mainly selected based on the following principals:

1. It must be dimensionless.
2. It should reflect the effect of interact between the local stresses.
3. It must take into consideration the effect of variation of both, stress ratio (R) and the (A/B) ratio.

The earlier discussion had led us to suggest introducing the following form of failure criteria;

$$\left(\frac{\sigma_1}{F_1}\right)^2+\left(\frac{\sigma_2}{F_2}\right)^2+\left(\frac{\sigma_6}{F_6}\right)^2+K_1\left(\frac{\sigma_1\sigma_2}{F_1F_2}\right)+K_2\left(\frac{\sigma_1\sigma_6}{F_1F_6}\right)+K_3\left(\frac{\sigma_2\sigma_6}{F_2F_6}\right)=R.D$$

Where K_1, K_2, and K_3 are obtained from the results of the experimental work to maintain the RD equal the unity. The values of RD after modification, according to eq. (6-15, were plotted against the number of cycles to failure as shown in figs. 21 and 22, for both fiber orientations.

The values of the constants K_1, K_2, and K_3 are proposed by:

$$K_1=-0.003\left(\frac{A}{B}\right)+12.5(R)+10$$

$$K_2=-1.97\left(\frac{A}{B}\right)^2+5.27\left(\frac{A}{B}\right)-0.37(R)-2.6$$

$$K_3=-0.33\left(\frac{A}{B}\right)-11.4(R)-8$$

5. Final conclusions

Fatigue tests of woven-roving glass fiber-reinforced polyester specimens, with $[0, 90]_2$ and $[\pm45]_2$ orientations, under combined bending and torsional moments, in phase, with different mean stresses resulted in the following conclusions:

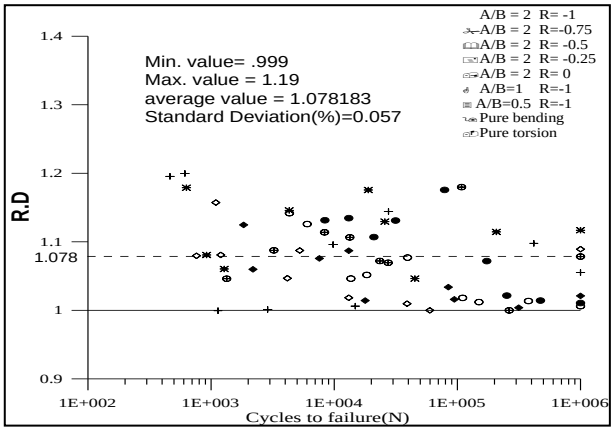

Fig. 21. RD of the modified failure criteria for the $[0,90]_2$ specimens

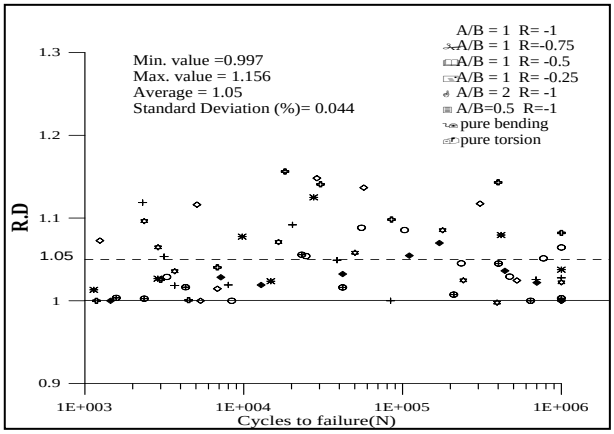

Fig. 22. RD of the modified failure criteria for the $[\pm45]_2$ specimen.

1. The $[\pm45]_2$ woven-roving GFRP is more fatigue resistant in torsion than the $[0,90]_2$.
2. The $[0, 90]_2$ woven-roving GFRP is more fatigue resistant in bending than the $[\pm45]_2$.
3. Using the power formula $\sigma_{max.} = a\,N^b$ has proved its suitability for $[0, 90]_2$ and $[\pm45]_2$ specimens subjected to combined bending and torsional moments with different mean stresses. And the value of the constant (a) was found to depend on the (A/B) ratio for both fiber orientations, with high correlation factor, according to the following equations:

$$a_{[0,90]_2}=16.08Ln(\frac{A}{B})+67.07$$

$$a_{[\pm45]_2}=13.61Ln(\frac{A}{B})+69.88$$

4. The form as Goodman's equation $\left\{\frac{\sigma_m}{S_u}+\frac{\sigma_a}{S_f}=1\right\}$ is suitable for representing the effect of the mean stress for both orientations, $[0, 90^o]_2$ and $[\pm 45^o]_2$, under combined bending and torsional fatigue loading.

1. A new form of failure criteria was introduced to govern the fatigue behavior of woven-roving GFRP under combined bending and torsional fatigue loading with both fiber orientations, $[0, 90]_2$ and $[\pm 45]_2$, as following:

$$\left(\frac{\sigma_1}{F_1}\right)^2+\left(\frac{\sigma_2}{F_2}\right)^2+\left(\frac{\sigma_6}{F_6}\right)^2+K_1\left(\frac{\sigma_1\sigma_2}{F_1F_2}\right)+K_2\left(\frac{\sigma_1\sigma_6}{F_1F_6}\right)+K_3\left(\frac{\sigma_2\sigma_6}{F_2F_6}\right)=R.D$$

And K_1, K_2, and K_3 are constants obtained from the experimental work, depending on the values of (R) and (A/B) ratios.

$$K_1=-0.003\left(\frac{A}{B}\right)+12.5(R)+10$$

$$K_2=-1.97\left(\frac{A}{B}\right)^2+5.27\left(\frac{A}{B}\right)-0.37(R)-2.6$$

$$K_3=-0.33\left(\frac{A}{B}\right)-11.4(R)-8$$

References

[1] S.S. Wang, E.S.M. Chim, .F. Socie, J. V. Gauchel and J.L. Olinger "Tensile and Torsional Fatigue of Fiber-Reinforced Composites at Cryogenic Temperatures", J. of Engineering Materials and Technology, April, Vol. 104, pp. 121-127 (1982).

[2] E. Krempl, D.M. Elzey, B.Z. Hong, T., Ayar and R.G. Loewy. "Uniaxial and Biaxial fatigue Properties of Thin-Walled Composite Tubes", J. of the American Helicopter Society, August, pp. 3-10 (1988).

[3] A.A. El-Midany "Fatigue of Woven-Roving Glass Fibre Reinforced Polyester under Combined Bending and Torsion", PhD. Thesis, Alexandria University-Egypt (1995).

[4] A. BradelyLerch "Model Determined for Predicting Fatigue Lives of Metal Matrix Composites under Mean Stresses", (www.grc.nasa.gov).

[5] N.A. Mohamed "The Effect of Mean Stress on the Fatigue Behaviour of Woven-Roving GFRP Subjected to Torsional Moments", MSc. Thesis, Alexandria University-Egypt (2002).

[6] A.K. Jihad, "Delamination Growth of GFRE Composites under Cyclic Torsional Momoents", PhD. Thesis, Alexandria University-Egypt (2001).

[7] M. Mohamed Yousef "The Inclusion Effect on the Fatigue Behaviour of Woven-Roving GRP Composite Materials", MSc. Thesis, Alexandria University-Egypt (2001).

[8] A.I. Sharara "Effect of Stress Ratio on Fatigue Characteristics of Woven-Roving Glass Reinforced Polyester", MSc. Thesis, Alexandria University-Egypt (1997).

[9] M.N. Abouelwafa, A.H. Hamdy and E.A. Showaib "A New Testing Machine for Fatigue Under Combined Bending and Torsion Acting Out-of phase", Alexandria Engineering Journal, Vol. 28 (4), pp. 113-130 (1989).

[10] Ramesh Talreja "Fatigue of Composite Materials", Technomic Publishing Co., Inc., (ISBN: 87762-516-6) (1987).

[11] M. James, Whitney, Isaac M. Daniel, and R. Byron Pipes "Experimental Mechanics of Fibre Reinforced Composite Materials", The Society of Experimental Stress Analysis (1982).

Received March 27, 2007
Accepted May 22, 2007